

LOW FREQUENCY, LOW β CAVITY PERFORMANCE IMPROVEMENT STUDIES

P. Kolb*, R.E. Laxdal, Z. Yao, TRIUMF, Vancouver, BC, Canada

Abstract

In recent years, new discoveries such as N₂ doping and infusion lead to significant increases in Q_0 and accelerating gradient for 1.3 GHz, $\beta = 1$ elliptical cavities. To understand and to adapt these treatments for lower frequency, $\beta < 1$ cavities, two coaxial test cavities, one quarter-wave resonator (QWR) and one half-wave resonator (HWR), have been built and put through a systematic study of these new treatments to show the effectiveness of these treatments at different frequencies. These cavities are tested in their fundamental mode and several higher order modes to study the frequency dependence of new cavity treatments such as N₂ doping and infusion. Results of these studies are presented.

INTRODUCTION

The performance of SRF cavities in terms of Q_0 and maximum reachable accelerating field continued to improve in recent years due to the discovery of surface treatments like high temperature degassing [1], N₂ doping [2], N₂ infusion [3], and two-step baking [4], environment control with flux expulsion utilizing a fast cooldown [5], and external field cancellation [6], and new materials like Nb₃Sn [7]. These discoveries were made exclusively on 1.3 GHz single cell elliptical cavities, which are widely used as testing cavities. TEM mode cavities on the other hand are generally less studied and have their own challenges with a well recognized, but not explained, medium field Q slope. Similarly, the influence of the geometry on Q_0 and characteristics like flux expulsion is poorly understood.

To evaluate how these new treatments perform at different frequencies and different geometries, two coaxial cavities were designed [8] and built to extend the range of investigated frequencies from 650-3900 MHz [9] down to frequencies commonly used in TEM mode cavities. These new multi-mode cavities can be driven in resonant modes ranging from 217 MHz to 1555 MHz to extract frequency dependency of the treatment without changing external variables like cooldown speed, magnetic field, surface roughness, and particulate contamination. These cavities can be viewed as basic TEM mode test units analogous to single cell 1.3 GHz cavities, to experiment with new treatments to improve the Q_0 and quench fields of TEM mode SRF cavities that see use in hadron accelerators.

METHODOLOGY

Cavities

Two coaxial cavities will be used for this study - one quarter wave cavity (QWR) and one half wave resonator

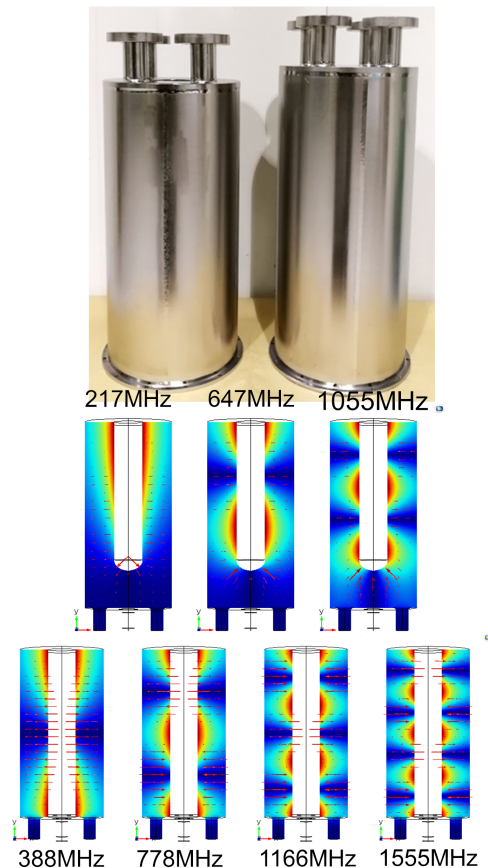


Figure 1: Photo and field distributions of the coaxial QWR and HWR test cavities.

(HWR). The frequencies of the TEM resonant modes of interest in the QWR are 217 and 648 MHz, while the modes of the HWR are at 388, 778, 1166 and 1555 MHz. The reduced frequency range of the QWR is due to the field distortion at the high voltage tip of the inner conductor that generates distorted peak surface fields compared to the pure coax geometry of the HWR. Unique to these cavities is the lack of beam ports, which would not have a purpose in these test cavities and would complicate fabrication. There are also no features or requirements to frequency tune the cavities.

The body of the cavities are made out of RRR niobium, while the port flanges are reactor grade niobium to reduce fabrication cost. The all niobium construction is done to avoid different materials than Niobium (NbTi, Stainless steel,...) to diffuse during high temperature heat treatment and potentially contaminate the cavity. All joints that make up the RF volume are electron beam welded. Both cavities have four ports on one side of the cavity as can be seen in

* kolb@triumf.ca

Content from this work may be used under the terms of the CC BY 3.0 licence (© 2019). Any distribution of this work must maintain attribution to the author(s), title of the work, publisher, and DOI.

Fig. 1. These ports are used for rinsing, vacuum connection, mounting the variable RF coupler, and the pick up antenna. Each cavity has its own coupler and pick-up. In the QWR, RF is coupled in via the electric field and in the HWR via the magnetic field.

The cavities are of similar size to 1.3 GHz single cell cavities and fit in TRIUMF's induction furnace, which was designed for heat treatments of single cell cavities. Hermetic sealing of the cavity ports is done via indium wire seals.

Processes

The test plan for both cavities consists of performance measurements at various points in the treatment plan. The baseline performance of the cavity is measured after a deep etch of 120 μm via BCP to remove the from fabrication damaged surface layer. The initial treatment schedule follows standard SRF cavity treatment protocols and are part of the treatment study and are done subsequently:

- 120 C bake for 48 h,
- degassing at 800 C for 6 h,
- flash BCP of 15 μm ,
- 120 C bake for 48 h.

After each treatment the performance of the cavity is measured. New treatments like infusion/doping will follow after these commonly used treatments are characterized.

After each treatment, the cavity is rinsed with HPR, assembled and hermetically sealed in a class 10 clean room environment. An exception to this is the 120 C bake, which is done in the cryostat without opening the cavity, eliminating the need for HPR and assembly. Evacuation of the RF space up to a rough vacuum of a few mTorr is done via controlled pumping at around 1 Torr/s or slower and is done while the cavity is still in the class 10 clean room. The cavity is then moved to the testing area and assembled with diagnostics (temperature sensors, fluxgate probes,...) on the cryostat insert. High vacuum in the cavity is established and maintained with active pumping via a turbo pump once the cavity is in the cryostat.

Typically a fast cooldown through the Q disease regime is done to limit the time between 200 and 50 K to the order of 1h 40min, although future studies will involve studying the role of cooldown speed and temperature gradient across the cavity with respect to either flux expulsion or hydride formation. Once the cryostat is filled with 4.2 K liquid helium, RF cables are calibrated and the cavity is conditioned for multipacting and field emission as needed. The RF is controlled via a self excited loop as described in [10]. Fixed temperature measurements of Q_0 as a function of B_p are done up to the quench field in continuous wave. Afterwards pulsed measurement are performed to determine the nature of the quench.

Once done with measurement of all modes at 4.2 K, a slow cooldown to 2.0 K begins, during which Q_0 data is taken as a function of temperature at fixed field amplitudes. This

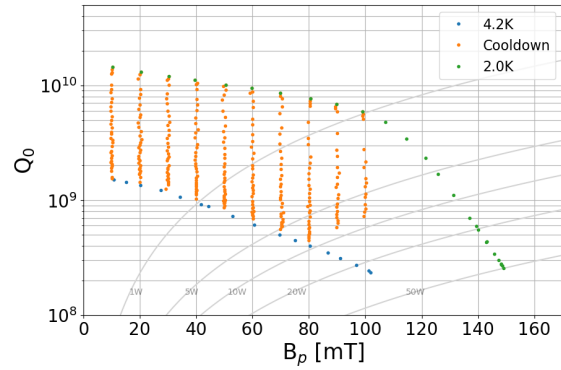


Figure 2: Q vs T measurement at different field amplitudes in the 217 MHz mode while cooling down from 4.2 K to 2.0 K.

data is taken to extract R_{BCS}^* and R_{res}^* at this field level via fitting the average $R_s^* = G/Q_0$ to

$$R_s^*(B_p, T) = R_{BCS}^*(B_p, T) + R_{res}^*(B_p) \quad (1)$$

$$= A(B_p)/T \cdot \exp\left(-\frac{\Delta(B_p)}{k_B T}\right) + R_{res}^*(B_p) \quad (2)$$

with A , Δ and R_{res}^* as fitting parameters. It should be noted that due to the field dependence of R_s^* and non-uniform field distribution of H (Fig. 1) the formula

$$R_s = G/Q_0 = \omega \mu_0 \frac{\int_V |\mathbf{H}|^2 dV}{\int_S |\mathbf{H}|^2 dS} / Q_0 \quad (3)$$

is not accurate. Steps to extract the true $R_s(B)$ dependence are noted below. To extract the field dependence of R_{BCS}^* and R_{res}^* , multiple Q_0 vs T curves in 10 mT steps up to 15-20 W power level are measured as is shown in Fig. 2.

The extracted field dependencies are then corrected for geometry effects to get the true R_{BCS} and R_{res} using correction factors for the field dependence coefficients based on the field distribution [11]. $R^*(B_p)$ can be generally expressed by a polynomial of form

$$R^* = \sum_i \alpha_i \cdot B_p^{x_i} \quad (4)$$

with coefficients α_i and in general any exponent x_i not limited to whole numbers. Depending on the EM field distribution of the mode in the resonator, the coefficients α_i need to be multiplied by correction factors depending on x_i to get the true R . As can be seen in table 1, both modes of the QWR have similar correction factors, leading to only small relative changes between QWR modes when converting R_s^* to R_s if the field dependence is similar. In comparison, an elliptical cavity has correction factors all close to unity due to its fairly uniform field distribution over the RF surface.

High temperature heat treatments are done in TRIUMF's induction furnace, which is able to work with low pressure

Table 1: Field Dependence Correction Factors for the QWR

| x | 217 MHz | 648 MHz |
|---|---------|---------|
| 0 | 1 | 1 |
| 1 | 1.432 | 1.473 |
| 2 | 1.778 | 1.871 |

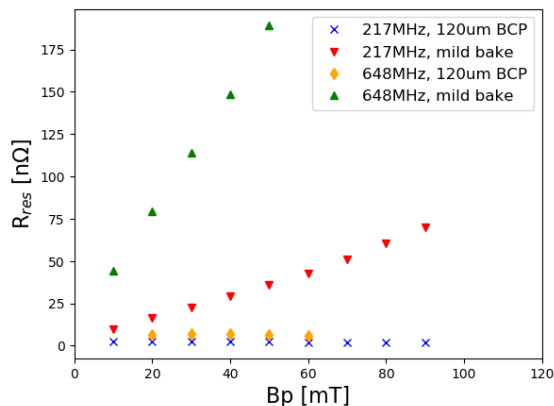


Figure 3: After the initial 120C mild bake, the cavity showed Q disease like behavior which is observed in R_{res}^* with a strong, linear field dependence.

gasses for N2 infusion and doping, and is dedicated to treating solely components made out of niobium. The initial hydrogen degassing treatment of the QWR was at 800 C for 6 hours.

RESULTS

So far, several surface treatments and subsequent performance measurements have been performed on the QWR, which can be operated in resonant modes at 217 and 648 MHz.

In this paper, results at the two frequencies after the baseline preparation, 800 C degass and flash BCP, and 120 C bake are reported. The initial 120 C bake did not improve the performance as Q disease caused by extended time in the critical temperature regime during warm-up allowed hydrides to form and persist during the mild bake. The Q disease introduced a strong, linear field dependence of R_{res}^* in both modes, with seemingly stronger slope at higher frequency as can be seen in Fig. 3. More data at different frequencies is needed to make conclusions about the nature of this increased slope.

Following the degassing, the low field Q_0 recovered, but showed a Q drop behavior at low to moderate field levels. This was caused by contamination of the RF surface during the degassing process, presumably from indium seal residue on the Nb flanges that migrated into the RF surface.

After a flash BCP treatment of 15 μm , the baseline performance is recovered as is shown in Fig. 4 for 4.2 K and Fig. 5 for 2.0 K. This is observed for both modes, with a slight increase in performance at higher fields in the 648 MHz mode. The degradation of Q_0 at high fields in the 2.0 K mea-

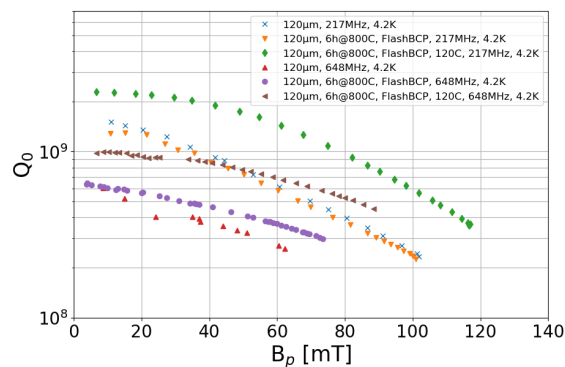


Figure 4: Q_0 at 4.2 K of the QWR. After degassing and flash BCP, the cavity performance is unchanged compared to the baseline performance in both modes. After an additional 120C bake the Q improves significantly at 4.2 K.

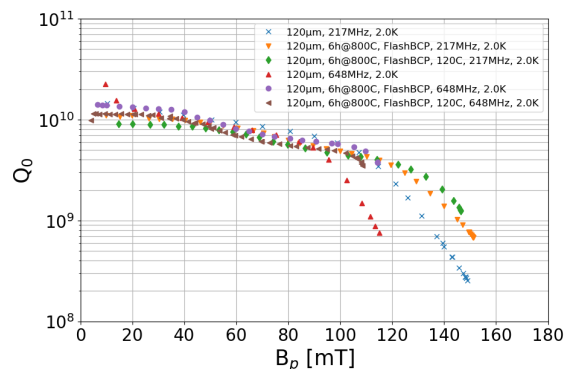


Figure 5: Q_0 at 2.0 K of the QWR. The low to medium field performance does not show any changes regardless of treatment in both modes. Improvements at high field are due to decreased field emissions.

surements is caused by field emissions. After a dedicated soak of the cavity at around 100 K for approximately 3 days, the cavity performed at the same levels, showing that the degassing worked as intended.

The following 120 C bake for 48 h increases Q_0 in both modes at 4.2 K significantly as can be seen in Fig. 4, while at 2.0 K the Q_0 is unchanged. This indicates that the bake reduces R_{BCS} while leaving R_{res} at the same levels. By normalizing the average R_s^* to a low field value, the field dependency independent of frequency is shown in Fig. 6. Up to medium field levels only minor changes in slope character can be observed, independent of mode, temperature, and surface treatment.

In all shown cases the field limiting quench at 4.2 K is caused by the limited cooling capacity of the inner conductor, while at 2.0 K the limitation is field emissions.

Separating the two components of the surface resistance by using the Q_0 data taken during the cooldown to 2.0 K, shows this as a clear reduction in R_{BCS}^* as can be seen in Fig. 7 and Fig. 8 for 4.2 K and 2.0 K respectively, while the temperature independent R_{res}^* (Fig. 9) slightly increases with the bake.

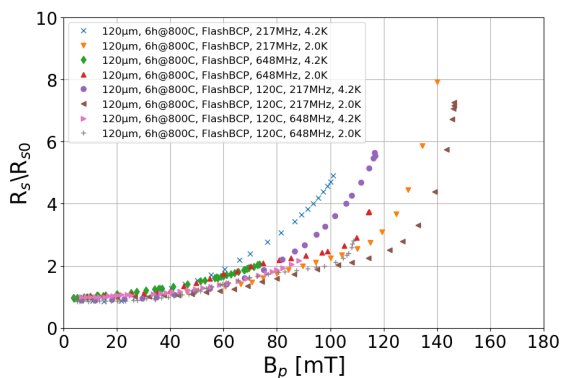


Figure 6: Normalized average R_s of the QWR shows a general similar trend of R_s^* as field increases, no matter the treatment, frequency or temperature.

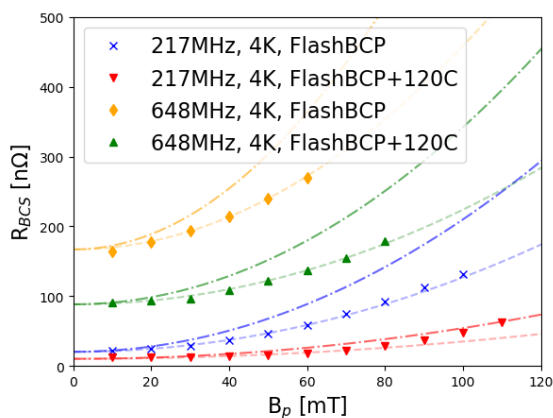


Figure 7: R_{BCS}^* ($T=4.2$ K)[markers] as a function of field before and after the 120 C bake with quadratic fits [dashed line] and geometry corrected fit [dash-dotted line]. The bake clearly reduces the BCS component both in magnitude and in field dependence.

In low to mid field amplitude, R_{BCS}^* follows a quadratic increase with field that can be fitted to

$$R_{BCS}^* = R_{BCS,0} + \gamma \cdot B_p^2 \quad (5)$$

with the fit parameters $R_{BCS,0}^*$ as the zero field BCS resistance and γ as slope parameter. These fits are shown in Fig. 7 and 8. At high fields, deviations from the fit are likely caused by limited cooling capacity above 2.17 K and the resulting additional losses due to surface heating.

The temperature independent residual resistance R_{res}^* on the other hand follows a mostly linear trend in both resonant modes that can be fitted to

$$R_{res}^* = R_{res,0} + R_{res,1} \cdot B_p \quad (6)$$

with the fit parameters $R_{res,0}^*$ as the zero field residual resistance and $R_{res,1}$ as slope. As can be seen in Fig. 9, in both modes the bake increases $R_{res,0}$ while the slope stays

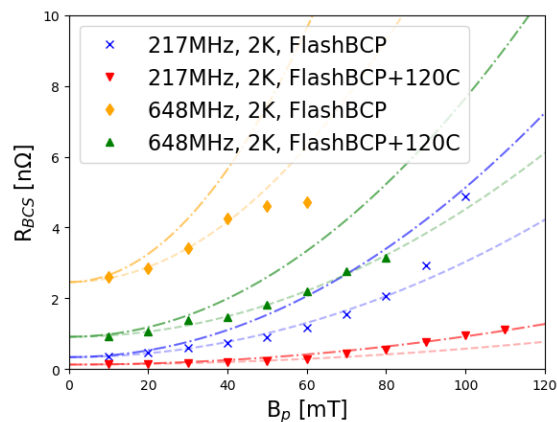


Figure 8: R_{BCS}^* ($T=2.0$ K)[markers] as a function of field before and after the 120 C bake with quadratic fits [dashed line] and geometry corrected fit [dash-dotted line]. Similar to 4.2 K, R_{BCS} is reduced by the bake in its magnitude and field dependence.

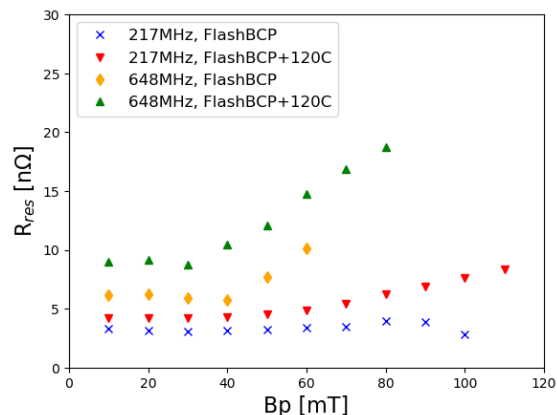


Figure 9: The temperature independent R_{res}^* increases slightly with the 120 C bake in both frequencies. The higher frequency mode increases in R_{res}^* slightly more than the lower frequency mode.

fairly similar to before the bake. In the 648 MHz, mode at around 30 to 40 mT, a stronger slope appears, which could indicate a small defect on the surface in an area of high magnetic field for the 648 MHz mode and a low field area for the 217 Mhz mode.

Figures 10 and 11 show the R_{BCS} fitting parameters A and Δ/k_p as function of field with normalized versions in Figures 12 and 13 respectively. The bake seems to decrease A while increasing Δ in magnitude. The normalized field dependency plots show that the coefficient A seems to follow an upward trend with increasing field amplitude, while Δ trends towards lower values. The bake decreases the field dependence of A while no clear effect can be seen on the field dependence of the energy due to the bake.

Content from this work may be used under the terms of the CC BY 3.0 licence (© 2019). Any distribution of this work must maintain attribution to the author(s), title of the work, publisher, and DOI.

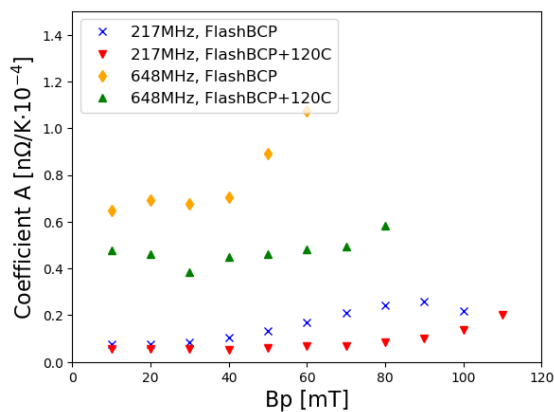


Figure 10: Fitting parameter A of R_{BCS}^* as a function of field before and after the 120 C bake.

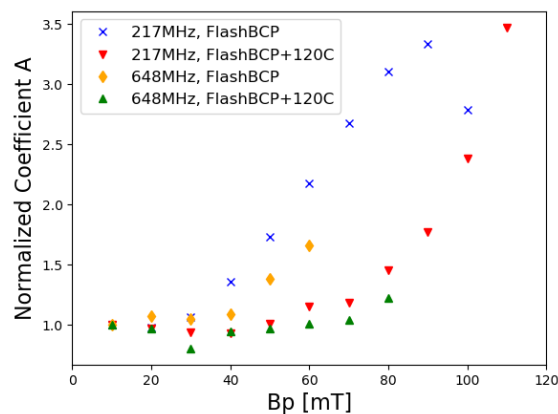


Figure 12: Normalized fitting parameter A of R_{BCS} as a function of field before and after the 120 C bake.

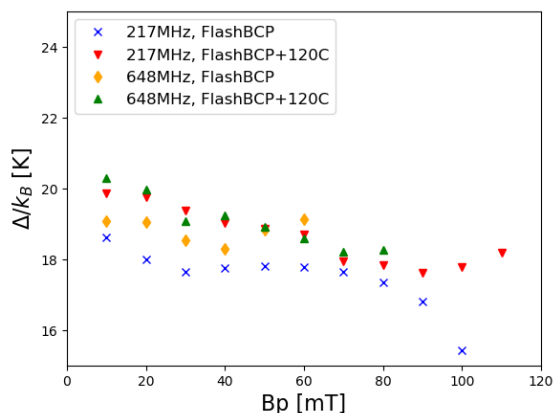


Figure 11: Energy gap Δ/k_B as a function of field before and after the 120 C bake.

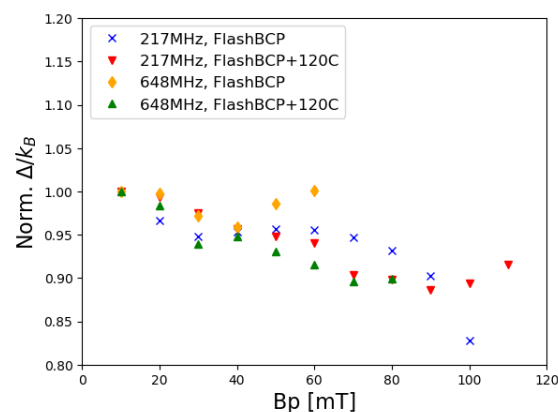


Figure 13: Normalized energy gap Δ/k_B as a function of field before and after the 120 C bake.

CONCLUSION

Studies to determine the frequency dependence of surface resistance in coaxial SRF cavities are under way and several performance measurements with different treatments of the QWR have been shown. The 120 C bake for 48 h reduces R_{BCS} significantly for both investigated frequencies, while slightly increasing R_{res} . This behavior is similar to studies done on 1.3 GHz cavities and is due to a reduction of the mean free path at the surface towards a more optimized R_{BCS} . This treatment shows its significant benefit if the cavity is operating at 4.2 K. At this temperature, R_{BCS} is the dominant contribution to R_S at frequencies typical for QWR and HWR cavities. At 2.0 K the overall performance is fairly unchanged by the bake. The effects of the 120 C bake on the R_{BCS} coefficients A and Δ and their field dependency are presented. The bake reduces both the magnitude and field dependency of A , while Δ is increased in magnitude while its field dependency seems unchanged.

The next step in the treatment chain for the QWR will be N2 infusion investigate the effects of this treatment on coaxial cavities. Multiple resonant modes will be used to determine the response of this treatment to different frequen-

cies. Dedicated studies to optimize the infusion recipe are planned to study the behavior of this treatment at low frequencies. Studies using the HWR are commencing in the near future which will allow further insight in the frequency dependency. N2 doping requires electro-polishing post doping and efforts to develop EP techniques for the test cavities are starting.

Simultaneously, work is going on to include flux expulsion studies using a 3D Helmholtz coil assembly. These will be used to either cancel the background magnetic field completely or to enhance it to specific values to study the flux expulsion behavior of coaxial cavities under different cooldown scenarios and measure the sensitivity of coaxial cavities to external magnetic fields.

ACKNOWLEDGMENTS

The authors would like to acknowledge the incredible help from our technical team, without whom all of this would not have been possible.

REFERENCES

- [1] A. Grassellino *et al.*, “Fermilab experience of post-annealing losses in SRF niobium cavities due to furnace contamination and the ways to its mitigation: a pathway to processing simplification and quality factor improvement”, arXiv:1305.2182.
- [2] A. Grassellino *et al.*, “Nitrogen and argon doping of niobium for superconducting radio frequency cavities: a pathway to highly efficient accelerating structures”, *Supercond. Sci. Technol.* vol. 26 p. 102001, 2013. doi:10.1088/0953-2048/26/10/102001
- [3] A. Grassellino *et al.*, “Unprecedented quality factors at accelerating gradients up to 45MVm^{-1} in niobium superconducting resonators via low temperature nitrogen infusion”, *Supercond. Sci. Technol.* vol. 30, p. 094004, 2017. doi:10.1088/1361-6668/aa7afe
- [4] A. Grassellino *et al.*, “Accelerating fields up to 49 MV/m in TESLA-shape superconducting RF niobium cavities via 75C vacuum bake”, arXiv:1806.09824.
- [5] J.-M. Vogt, O. Kugeler, and J. Knobloch, “Impact of cooldown conditions at T_c on the superconducting rf cavity quality factor”, *Phys. Rev. ST Accel. Beams* vol. 16, p. 102002, 2013. doi:10.1103/PhysRevSTAB.16.102002
- [6] A. Romanenko *et al.*, “Dependence of the residual surface resistance of superconducting radio frequency cavities on the cooling dynamics around T_c ”, *J. Appl. Phys.* vol. 115, p. 184903, 2014. doi:10.1063/1.4875655
- [7] S. Posen and M. Liepe, “RF Test Results of the first Nb3Sn Cavities Coated at Cornell”, in *Proc. SRF'13*, Paris, France, Sep. 2013, paper TUP087, pp. 666–669.
- [8] Z. Y. Yao, T. Junginger, R. E. Laxdal, B. Matheson, B. S. Waraich, and V. Zvyagintsev, “Design of Multi-frequency Coaxial Test Resonators”, in *Proc. SRF'17*, Lanzhou, China, Jul. 2017, pp. 531–534. doi:10.18429/JACoW-SRF2017-TUPB065
- [9] M. Martinello *et al.*, “Anti-Q-slope enhancement in high-frequency niobium cavities”, in *Proc. IPAC'18*, Vancouver, Canada, Apr.-May 2018, pp. 2707–2709. doi:10.18429/JACoW-IPAC2018-WEPML013
- [10] Z. Y. Yao *et al.*, “Tests of Multi-frequency Coaxial Resonators”, in *Proc. LINAC'18*, Beijing, China, Sep. 2018, pp. 420–422. doi:10.18429/JACoW-LINAC2018-TUP0040
- [11] J.R. Delayen, H. Park, S.U. De Silve, G. Ciovati, and Z. Li, “Determination of the magnetic field dependence of the surface resistance of superconductors from cavity tests” *Phys. Rev. Accel. Beams*, vol. 21, p. 122001, 2018. doi:10.1103/PhysRevAccelBeams.21.122001